Electronic transport properties in random one-dimensional chains containing mesoscopic-ring defects

X. Huang
CCAST (World Laboratory), P. O. Box 8730, Beijing 100080, China
and Optical Communication Researching Section, Communication Engineering Institute of Nanjing, PLA University of Science and Technology, Nanjing 210016, China
(Received 19 April 1999)

We study the electronic transport properties in one-dimensional systems with two kinds of mesoscopic ring defects: squarelike mesoscopic ring (SMR) defects and siamese-twins-like mescoscopic ring (STMR) defects. By using the transfer-matrix method, the resonant energies (where the transmission coefficient $T=1$) are derived successfully for both system. For the one SMR defect system, two resonant energies are found as a function of the magnetic flux Φ threading the ring defect, while for the latter case, two magnetic-flux-dependent and one magnetic-flux-independent resonant energies are predicted in the system, furthermore, if Φ takes some specific values, one of the Φ-dependent resonant energies may be the same as the Φ-independent resonant energy. The word ''resonant'' is used to describe this situation. When a finite concentration of SMR or STMR defects are randomly embedded in a perfect chain, the numerical results confirm all the analytical predictions. Finally, for the ''resonant'' case, we show numerically a rather wide perfect transmission region which is almost ten times as wide as that of the ''unresonant'' case. [S0163-1829(99)03438-4]

I. INTRODUCTION

The progress of fabrication technology in semiconductors and related areas allows people to fabricate devices at a rather small size, the so-called mesoscopic system, and the quantum transport in mesoscopic systems is of considerable current interest.[1–30] In such mesoscopic systems, the phase coherence length of electrons becomes large compared to the system dimension, thus the system can be modeled as a phase-coherent elastic scattering. For the mesoscopic systems, the persistent current of isolated rings has been the focus of attention.[3,4] As for open-ring systems, many theoretical works have been devoted to the investigation of the electronic properties of the systems within the framework of the waveguide theory.[9,13,14,17] In addition, the transmission of electrons through open mesoscopic ring systems has been studied within the tight-binding model.[8,15,25,26] It should be noted that most of the mentioned works have been limited in the ideal mesoscopic systems, in which the interactions such as electron-electron (e-e), electron-phonon (e-p) interaction are ignored. Later, the effects of e-e interaction have been considered by many groups.[16,18,19] Disorder in the mesoscopic systems is also studied by many authors.[20–22] Recently, the interaction of e-p in the mesoscopic system has been studied by introducing the nonlinear impurities.[24] Otherwise, in these studies, some mesoscopic ring with special loop structures have been considered, for example, the multiring system in parallel,[25] multiply connected normal conductor loop,[17] and open necklace of loop geometry.[20] Recently, some works concerning the coherent transport in a multiterminal mesoscopic Aharonov-Bohm ring with a quantum dot embedded in an arm have been experimentally and theoretically studied and some interesting results have been reported.[27–30]

On the other hand, it is well known that all the electronic states are localized even for infinitesimal disorder in a one-dimensional lattice.[31] However, during the last decade analytical and numerical studies revealed that delocalized states can exist in one-dimensional lattices with short-range correlations.[32–37] In 1990, the simplest and successful one-dimensional random dimer model (RDM) was introduced and studied.[32] In this model, the on-site energy takes two possible values ϵ_A, ϵ_B, and the same value of site energy is assigned at random to two succeeding lattice sites. It has been argued that $\sqrt{N}$ eigenstates have a localization length longer than the length of the finite sample, provided that $|\epsilon_A-\epsilon_B|\leqslant 2V$, where V is the nearest-neighbor matrix element. The reason for the occurrence of the delocalization phenomenon in RDM has been attributed to the existence of the symmetric internal structure of RDM.[34] In the later works, some defects with different structure have been introduced and studied. Examples of these models are the (1) random n-mer model, (2) repulsive binary alloy, (3) random bipolaron lattice, and (4) random dimer-trimer model.[34–37] The common ingredient these models share is that the random defects possess internal structure that is symmetric about some plane.

To the best of our knowledge, there is no work devoted to studying the influence of magnetic flux on the electronic transport properties in random systems. In this paper, we concentrate on investigating the electronic transport properties of one-dimensional chains made by the insertion of mesoscopic ring defects, which are threaded by magnetic flux. Consider a one-dimensional tight-binding model of a random binary alloy in which the site energies ε_a and ε_b are arranged as $\cdots\varepsilon_a\varepsilon_b\varepsilon_a\varepsilon_a\varepsilon_b\varepsilon_b\varepsilon_a\varepsilon_b\varepsilon_a\varepsilon_b\varepsilon_a\varepsilon_a\varepsilon_b\cdots$. To explore the effect of magnetic flux on this system, we assume that all ε_b are replaced by mesoscopic loop defects with a symmetric internal structure. The questions are (i) When each loop is threaded by a magnetic flux Φ, does the magnetic field destroy the internal symmetric structure of mesoscopic loop defects? (ii) Do any new phenomena happen because of the

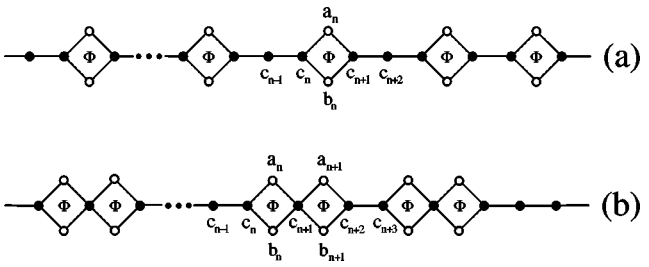

FIG. 1. The scheme of random lattices with different defects: (a) squarelike mescoscopic ring (SMR) defects, (b) siamese-twins-like mescoscopic ring (STMR) defects.

introduction of the magnetic field?

In this paper, we aim to answer the two questions raised above. The paper is organized as follows. In Sec. II, first, we introduce the two theoretical modes we are studying, second, we present the formalism for analyzing and calculating the transmission coefficient of the studied models. In Sec. III, when a mesoscopic loop defect is embedded in a perfect lattice, we derive exactly the resonant energies for the model through a transfer-matrix technique. Then, in Sec. IV, we perform numerical simulations of a transmission coefficient for the case when a finite concentration of defects are randomly added. Finally, Sec. V, is devoted to a discussion of our results and gives a summary.

II. MODEL

We start with a tight-binding monatomic chain, for which the site energy is ε_a and atoms are connected by a same hopping interaction V. In this paper, we consider two types of defects which are randomly inserted in the host chain. The specific models (shown in Fig. 1) are the models with (a) squarelike mesoscopic ring (SMR) defects [see Fig. 1(a)], (b) Siamese-twins-like mesoscopic ring (STMR) defects [see Fig. 1(b)]. It is evident from Fig. 1 that these defects possess symmetric internal structure. In both cases, we assume that only the rings are threaded by a magnetic flux Φ.

In the tight-binding and nearest-neighbor interaction approximation, it is easy to write the equations for the wave amplitudes for the sites around the ring defect. For the nth SMR defect of Fig. 1(a), one has

$$\begin{aligned}
(E-\varepsilon_a)c_n &= Vc_{n-1}+Ve^{i\gamma/4}b_n+Ve^{-i\gamma/4}a_n,\\
(E-\varepsilon_b)a_n &= Ve^{i\gamma/4}c_n+Ve^{-i\gamma/4}c_{n+1},\\
(E-\varepsilon_b)b_n &= Ve^{-i\gamma/4}c_n+Ve^{i\gamma/4}c_{n+1},\\
(E-\varepsilon_a)c_{n+1} &= Ve^{-i\gamma/4}b_n+Ve^{i\gamma/4}a_n+Vc_{n+2},
\end{aligned} \tag{1}$$

while for the case of the STMR defect of Fig. 1(b), the equation is a little different:

$$\begin{aligned}
(E-\varepsilon_a)c_n &= Vc_{n-1}+Ve^{i\gamma/4}b_n+Ve^{-i\gamma/4}a_n,\\
(E-\varepsilon_b)a_n &= Ve^{i\gamma/4}c_n+Ve^{-i\gamma/4}c_{n+1},\\
(E-\varepsilon_b)b_n &= Ve^{-i\gamma/4}c_n+Ve^{i\gamma/4}c_{n+1},\\
(E-\varepsilon_a)c_{n+1} &= Ve^{-i\gamma/4}b_n+Ve^{i\gamma/4}a_n+Ve^{i\gamma/4}b_{n+1}\\
&\quad +Ve^{-i\gamma/4}a_{n+1},\\
(E-\varepsilon_b)b_{n+1} &= Ve^{-i\gamma/4}c_{n+1}+Ve^{i\gamma/4}c_{n+2},\\
(E-\varepsilon_b)a_{n+1} &= Ve^{i\gamma/4}c_{n+1}+Ve^{-i\gamma/4}c_{n+2},\\
(E-\varepsilon_a)c_{n+2} &= Ve^{-i\gamma/4}b_{n+1}+Ve^{i\gamma/4}a_{n+1}+Vc_{n+3}.
\end{aligned} \tag{2}$$

Here a_n and b_n are the site amplitude of the lower arm, the upper arm for ring n, ε_b is the site energy of the lower and upper arm, and $\gamma=2\pi\Phi/\Phi_0, \Phi_0=h/e$. Equations (1) and (2) can be rewritten in the matrix form

$$\begin{bmatrix} c_{n+1} \\ c_n \end{bmatrix} = \underline{P}^{(n)} \begin{bmatrix} c_n \\ c_{n-1} \end{bmatrix}, \tag{3}$$

where $\underline{P}^{(n)}$ is the promotion matrix which connects the adjacent site amplitudes c_n and $c_{n\pm1}$.

In general for a defect which occupies m sites, then the total promotion matrix across the defect is $\underline{P}_m = \underline{P}^{(n+m)}\underline{P}^{(n+m-1)}\cdots\underline{P}^{(n)}$. To study the problem of the transmission properties through the defect, we can write the the wave-function amplitudes to both sides of the defect as a single Bloch wave specified by a wave vector k.

$$c_j = \begin{cases} e^{ikj}+re^{-ikj} & \text{for } j\leqslant n, \\ te^{ikj} & \text{for } j\geqslant n+m. \end{cases} \tag{4}$$

For a given $\underline{P}_m$ and k, Wu *et al.*[34] have found the reflection amplitude r

$$r = -Z^{2n}\frac{\alpha^T\Gamma\underline{P}_m\alpha}{\alpha^T\Gamma\underline{P}_m\alpha^*}, \tag{5}$$

where

$$Z=e^{ik}, \Gamma=\begin{bmatrix} 0 & 1 \\ -1 & 0 \end{bmatrix}, \alpha=\begin{bmatrix} Z \\ 1 \end{bmatrix},$$

and α^T, is the transpose of α.

The condition for resonant energy E of the defect can be stated by saying the reflection amplitude r of Eq. (5) will vanish for the corresponding energy. Because E is the energy of the ordered band, it is limited by the following equation:

$$E-\varepsilon_a = 2V\cos k. \tag{6}$$

Then, it is evident that the whole energy band of the ordered lattice ranges from $[E_L, E_R]=[-2V+\varepsilon_a, 2V+\varepsilon_a]$.

When a large number of such defects are randomly placed in the host chain, the transmission properties can be investigated by direct numerical computation of the reflection or transmission coefficients through the transfer-matrix method. Generally, we can first consider electronic transmission through a one-dimensional chain of length N. We embed this chain in an infinite perfectly ordered atom chain. Then, in the conducting region to the left and the right of the chain, the normalized wave functions can be written as

$$c_n = \begin{cases} e^{ikn}+f_re^{-ikn} & \text{for } -\infty<n\leqslant 1, \\ f_te^{ikn} & \text{for } N+1\leqslant n<\infty. \end{cases} \tag{7}$$

We define the transfer matrix $T(N)$ by

$$\begin{bmatrix} f_t \\ if_t \end{bmatrix} = T(N) \begin{bmatrix} 1+f_r \\ i(1-f_r) \end{bmatrix}, \tag{8}$$

where

$$T(N) = S^{-1} M(N) S, \tag{9}$$

$$S = \begin{bmatrix} \cos k & \sin k \\ 1 & 0 \end{bmatrix}. \tag{10}$$

Note that $\det T(N) = 1$, thus, one can calculate the transmission coefficient in the relationship[38]

$$T = \frac{4}{2 + T(N)_{11}^2 + T(N)_{12}^2 + T(N)_{21}^2 + T(N)_{22}^2}. \tag{11}$$

We should point out that all our numerical results described below are obtained directly from Eq. (11).

III. ANALYTICAL CONCLUSIONS

A. A squarelike mesoscopic ring defect

Consider now the the model shown in Fig. 1(a). First we suppose only one SMR defect is embedded at site n in an otherwise perfect lattice. From Eq. (1), the relation of the site amplitudes which connects both ends of the defect is

$$\begin{bmatrix} c_{n+2} \\ c_{n+1} \end{bmatrix} = \underline{P}_s \begin{bmatrix} c_n \\ c_{n-1} \end{bmatrix} = \underline{M}_{n+1} \underline{M}_n \begin{bmatrix} c_n \\ c_{n-1} \end{bmatrix}, \tag{12}$$

where $\underline{P}_s$ is the total promotion matrix.

From Eqs. (1) and (3) one obtains

$$\underline{M}_n = \begin{bmatrix} \dfrac{(E-\varepsilon_a)(E-\varepsilon_b) - 2V^2}{2V^2 \cos(\gamma/2)} & -\dfrac{(E-\varepsilon_b)}{2V\cos(\gamma/2)} \\ 1 & 0 \end{bmatrix} \tag{13}$$

and

$$\underline{M}_{n+1} = \begin{bmatrix} \dfrac{(E-\varepsilon_a)(E-\varepsilon_b) - 2V^2}{V(E-\varepsilon_b)} & -\dfrac{2V\cos(\gamma/2)}{(E-\varepsilon_b)} \\ 1 & 0 \end{bmatrix}. \tag{14}$$

Using Eqs. (13) and (14), we can rewrite the corresponding total promotion matrix $\underline{P}_s$ of Eq. (12) as

$$\underline{P}_s = A_s \begin{bmatrix} \dfrac{(E-\varepsilon_a)}{V} & -1 \\ 1 & 0 \end{bmatrix} + \begin{bmatrix} B_s(E) & 0 \\ 0 & C_s(E) \end{bmatrix}, \tag{15}$$

where

$$A_s(E) = \frac{(E-\varepsilon_a)(E-\varepsilon_b) - 2V^2}{2V^2 \cos(\gamma/2)}, \tag{16}$$

$$B_s(E) = \frac{2V\cos(\gamma/2)}{E-\varepsilon_b}[A_s^2(E) - 1] - \frac{(E-\varepsilon_a)A_s(E)}{V}, \tag{17}$$

$$C_s(E) = -\frac{(E-\varepsilon_b)}{2V\cos(\gamma/2)}. \tag{18}$$

From Eqs. (16)–(18), when energy E satisfies

$$E = E_{12}^s = \varepsilon_a \pm \sqrt{(\varepsilon_a - \varepsilon_b)^2 + 4V^2 \sin^2(\gamma/2)}, \tag{19}$$

Eq. (15) can be rewritten as

$$\underline{P}_s = A_{\pm}^s \begin{bmatrix} \dfrac{(E-\varepsilon_a)}{V} & -1 \\ 1 & 0 \end{bmatrix} + B_{\pm}^s \begin{bmatrix} 1 & 0 \\ 0 & 1 \end{bmatrix}, \tag{20}$$

where

$$A_{\pm}^s = \frac{2W^2 \pm 2W\sqrt{W^2 + \sin^2(\gamma/2)} - \cos\gamma}{\cos\gamma},$$

$$B_{\pm}^s = -\frac{W \pm \sqrt{W^2 + \sin^2(\gamma/2)}}{\cos\gamma},$$

$$W = \frac{\varepsilon_a - \varepsilon_b}{2V}.$$

Wu *et al.*[34] have pointed out that the reflection amplitude of Eq. (5) will vanish only when the total promotion matrix is proportional to (1) the unit matrix or (2) the promotion matrix for the ordered system (or some linear combination of both). Evidently, for the case of $E_{12}^s = \varepsilon_a \pm \sqrt{(\varepsilon_a - \varepsilon_b)^2 + 4V^2 \sin^2(\gamma/2)}$, the total promotion matrix of Eq. (15) in this model reduces to the linear combination of the unit matrix and the ordered system promotion matrix [see Eq. (20)]. Because of the restriction of Eq. (6), it is straightforward to verify that the perfectly transmitted electronic states E_{12}^s can be found in the studied system provided that

$$-\cos\left(\frac{\gamma}{2}\right) \leqslant W \leqslant \cos\left(\frac{\gamma}{2}\right). \tag{21}$$

B. A siamese-twins-like mesoscopic ring defect

Thus far, we have shown theoretically the resonant energies of one SMR defect system. In what follow, we will turn to study the transmission properties of Fig 1(b). Similarly, as the first step, we consider the case in which only one STMR defect is inserted into the ideal one-dimensional lattice. From Eqs. (2) and (3), it follows that the total transfer-matrix across the defect can be written as

$$\begin{bmatrix} c_{n+3} \\ c_{n+2} \end{bmatrix} = \underline{P}_{st} \begin{bmatrix} c_n \\ c_{n-1} \end{bmatrix} = \underline{M}_{n+2} \underline{M}_{n+1} \underline{M}_n \begin{bmatrix} c_n \\ c_{n-1} \end{bmatrix}, \tag{22}$$

where $\underline{P}_{st}$ is the total promotion matrix, and $\underline{M}_n, \underline{M}_{n+1}, \underline{M}_{n+2}$ are given by

$$\underline{M}_n=\begin{bmatrix}\dfrac{(E-\varepsilon_a)(E-\varepsilon_b)-2V^2}{2V^2\cos(\gamma/2)} & -\dfrac{(E-\varepsilon_b)}{2V\cos(\gamma/2)}\\ 1 & 0\end{bmatrix}, \tag{23}$$

$$\underline{M}_{n+1}=\begin{bmatrix}\dfrac{(E-\varepsilon_a)(E-\varepsilon_b)-4V^2}{2V^2\cos(\gamma/2)} & -1\\ 1 & 0\end{bmatrix}, \tag{24}$$

$$\underline{M}_{n+2}=\begin{bmatrix}\dfrac{(E-\varepsilon_a)(E-\varepsilon_b)-2V^2}{V(E-\varepsilon_b)} & -\dfrac{2V\cos(\gamma/2)}{(E-\varepsilon_b)}\\ 1 & 0\end{bmatrix}. \tag{25}$$

Using Eqs. (23)–(25), Eq. (22) can be represented as

$$\underline{P}_{st}=\underline{A}_{st}\begin{bmatrix}\dfrac{(E-\varepsilon_a)}{V} & -1\\ 1 & 0\end{bmatrix}+\begin{bmatrix}B_{st}(E) & 0\\ 0 & C_{st}(E)\end{bmatrix}, \tag{26}$$

where

$$A_{st}(E)=1-\frac{[(E-\varepsilon_a)(E-\varepsilon_b)-4V^2]A_s(E)}{2V^2\cos(\gamma/2)}, \tag{27}$$

$$B_{st}(E)=-\frac{[(E-\varepsilon_a)(E-\varepsilon_b)-2V^2]}{V(E-\varepsilon_b)}[A_{st}(E)+1], \tag{28}$$

$$C_{st}(E)=-\frac{(E-\varepsilon_b)[(E-\varepsilon_a)(E-\varepsilon_b)-4V^2]}{4V^3\cos^2(\gamma/2)}. \tag{29}$$

From Eqs. (27)–(29), it is quite easy to derive that, when

$$E_{12}^{st}=\varepsilon_a\pm\sqrt{(\varepsilon_a-\varepsilon_b)^2+4V^2\sin^2(\gamma/2)}, \tag{30}$$

Eq. (26) can be represented by the linear combination of the promotion matrix for the ordered system and the unit matrix as

$$\underline{P}_{st}=A_{\pm}^{st}\begin{bmatrix}\dfrac{(E-\varepsilon_a)}{V} & -1\\ 1 & 0\end{bmatrix}+B_{\pm}^{st}\begin{bmatrix}1 & 0\\ 0 & 1\end{bmatrix}, \tag{31}$$

where

$$A_{\pm}^{st}=1+A_{\pm}^{s}\left[\cos^{-1}\left(\frac{\gamma}{2}\right)-A_{\pm}^{s}\right],$$

$$B_{\pm}^{st}=-B_{\pm}^{s}\left[\cos^{-1}\left(\frac{\gamma}{2}\right)-A_{\pm}^{s}\right].$$

Furthermore, when

$$E_{34}^{st}=\frac{\varepsilon_a+\varepsilon_b\pm\sqrt{(\varepsilon_a-\varepsilon_b)^2+16V^2}}{2}, \tag{32}$$

we have

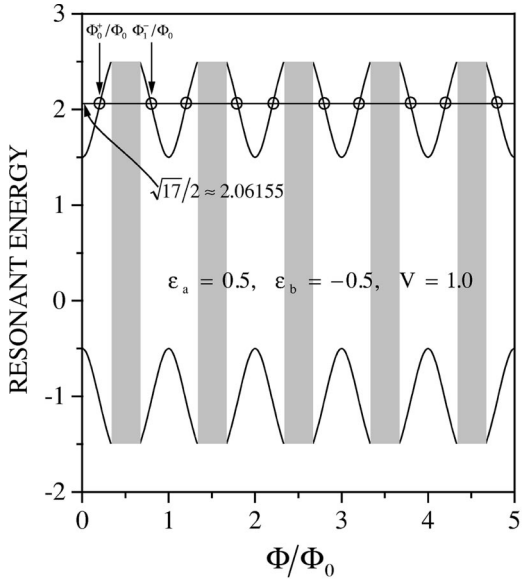

FIG. 2. The illustration of resonant energy vs Φ/Φ_0 for the STMR defect system. The open circles indicate the ''resonant'' energy cases there, two resonant energies are the same.

$$\underline{P}_{st}=\begin{bmatrix}\dfrac{(E-\varepsilon_a)}{V} & -1\\ 1 & 0\end{bmatrix}. \tag{33}$$

The analytical results of expressions (31) and (33) indicate that the energies E_{12}^{st} and E_{34}^{st} are the candidates of the resonant energy in the studied system, and the phenomenon of the vanishing of the reflection coefficients can be observed around these energies. It should be noted that the condition for the existence of these extended states is entirely determined by the system parameters $\varepsilon_a,\varepsilon_b,V$, and Φ. In fact, from the form of Eq. (30) it is clear that E_{12}^{st} are same as E_{12}^{s}, and then the condition that E_{12}^{st} exist in the studied system is also given by Eq. (21). In addition, E_{34}^{st} can be rewritten as

$$(E_{34}^{st}-\varepsilon_a)=V(-W\pm\sqrt{W^2+4}). \tag{34}$$

Consider the limitation of Eq. (21), we have

$$\begin{cases}|-W+\sqrt{W^2+4}|\leqslant 2\\ |-W-\sqrt{W^2+4}|\geqslant 2\end{cases},\quad \text{if } W\geqslant 0, \tag{35}$$

$$\begin{cases}|-W+\sqrt{W^2+4}|\geqslant 2\\ |-W-\sqrt{W^2+4}|\leqslant 2\end{cases},\quad \text{if } W\leqslant 0. \tag{36}$$

Equations (35) and (36) show that, for any given W, only one of the resonant energies E_{34}^{st} is allowed in the studied system (for simplicity, E_3^{st} is used to present the allowed resonant energy). To show more clearly the allowed resonant energies in the system, we plot in Fig. 2 the relationship between the, resonant energies (E_{12}^{st} and E_3^{st} of the STMR system) and the threading magnetic flux Φ. The figure is obtained under one set of special parameters $\varepsilon_a=0.5$, $\varepsilon_b=-0.5$, and $V=1.0$, corresponding to the case of $W>0$. As can be seen from the figure, there are two Φ-dependent resonant energies and one Φ-independent resonant energy, and in

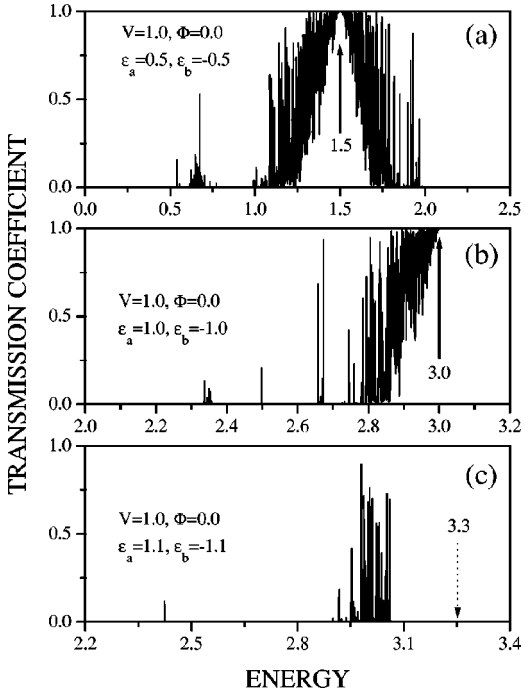

FIG. 3. Transmission coefficients as a function of the energy for the system of Fig. 1(a) with $N=5000$, and the magnetic flux $\Phi=0.0$. (a) and (b) show clearly one complete transmission peak. (c) As the parameters $(\varepsilon_a-\varepsilon_b)/2V=1.1>1.0$, then the resonant peak $E=3.3$ is not allowed.

some of the regions (marked by light gray), both magnetic-dependent resonant energies E_{12}^{st} are forbidden, consequently, only the magnetic-independent resonant energy appears in the figure. Interestingly, when Φ is chosen by some special values, two of the resonant energies are the same (for example, $E_1^{st}=E_3^{st}$ marked by an open circle in the figure), here we use the word resonant to describe this situation. Generally, suppose $W>0$, the resonant phenomenon takes place under the condition

$$\cos\gamma=\frac{(\varepsilon_a-\varepsilon_b)^2+(\varepsilon_a-\varepsilon_b)\sqrt{(\varepsilon_a-\varepsilon_b)^2+16V^2}}{4V^2}-1$$

$$=W^2+W\sqrt{W^2+4}-1. \tag{37}$$

If $|W^2+W\sqrt{W^2+4}-1|\leqslant 1$, from Eq. (37), one can obtain

$$\Phi_m^{\pm}=\Phi_0[m\pm\arccos(W^2+W\sqrt{W^2+4}-1)],$$
$$m=0,1,2\ldots. \tag{38}$$

Thus, the values of magnetic flux where the resonant energy happens are uniquely determined by Eq. (38). Expression (38) yields the conclusion that Φ_m^+/Φ_0 or Φ_m^-/Φ_0 has a period unity (see Fig. 2). Among each period, there are two values, the first two of them are given as

$$\Phi_0^+/\Phi_0=\arccos(W^2+W\sqrt{W^2+4}-1), \tag{39}$$

$$\Phi_1^-/\Phi_0=1-\arccos(W^2+W\sqrt{W^2+4}-1). \tag{40}$$

The above two special situations are marked in Fig. 2, we expect that some peculiar phenomenon can be observed at these points.

IV. NUMERICAL RESULTS

The main results are shown in Figs. 3 and 4 for the SMR defect systems, and in Figs. 5, 6, and 7 for the STMR defect systems. It should be noted that in all our numerical calculations given here, we fix the lattice site $N=5000$ and about half of these sites are randomly replaced by the mesoscopic ring defects.

A. Systems with many SMR defects

Figure 3 shows the transmission spectrum for different values of $\varepsilon_a-\varepsilon_b$: (a) $\varepsilon_a-\varepsilon_b=V=1.0$, (b) $\varepsilon_a-\varepsilon_b=2V=2.0$, and (c) $\varepsilon_a-\varepsilon_b=2.2V=2.2$. In the numerical calculations, we set the magnetic flux $\Phi=0$. As seen in Figs. 3(a)

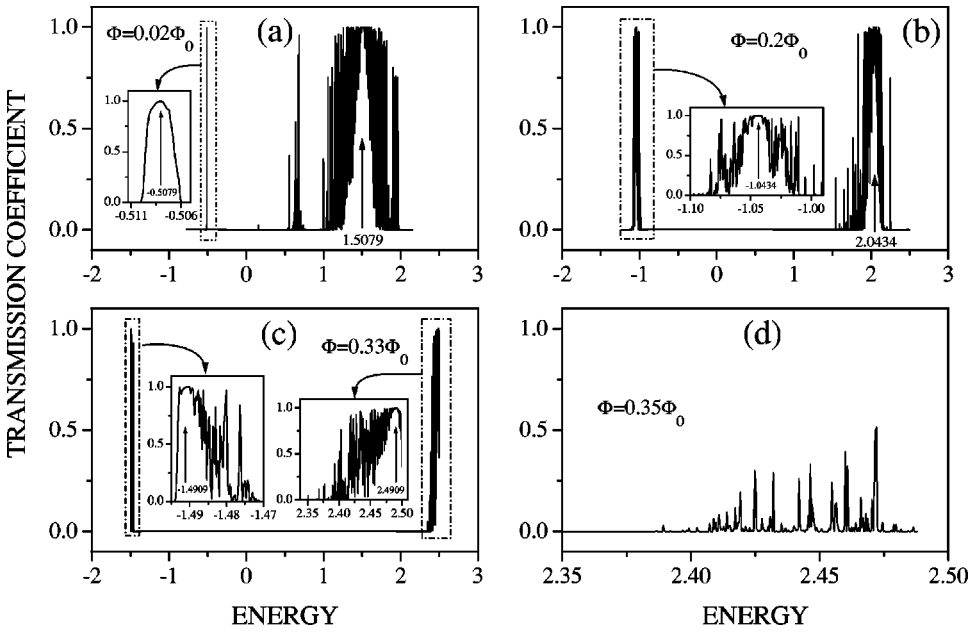

FIG. 4. Transmission coefficients as a function of the energy for the SMR defects system of Fig. 1(a) for different magnetic flux Φ. Other parameters are the same as those in Fig. 3(a). (a) $\Phi=0.02\Phi_0$, (b) $\Phi=0.2\Phi_0$, and (c) $\Phi=0.33\Phi_0$. In these three figures two resonant energies are clearly shown, and it can be seen that the resonant energies will move to the two edges of the energy band as the magnetic flux Φ increases. (d) $\Phi=0.35\Phi_0$, in this case, the resonant peak disappears.

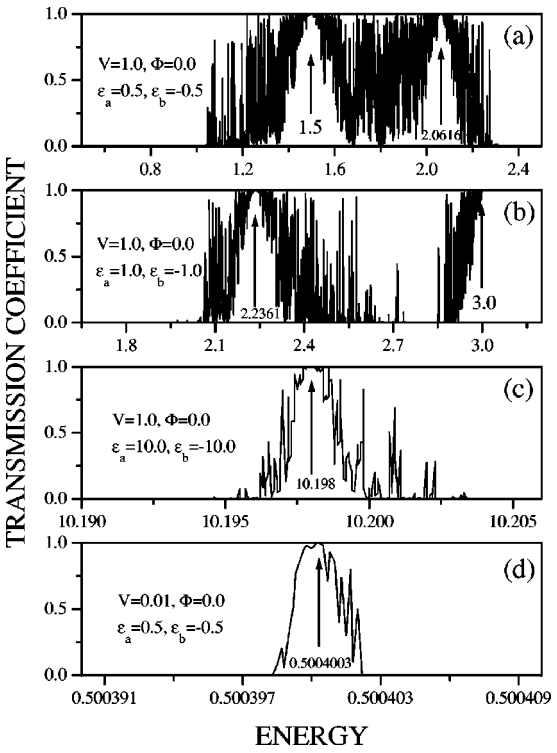

FIG. 5. Transmission coefficients as a function of the energy for the system of Fig. 1(b) with $N=5000$, and the magnetic flux $\Phi=0.0$. (a) and (b) show clearly two complete transmission peaks, respectively. (c) For a large parameter $\varepsilon_a=-\varepsilon_b=10.0$, and (d) for a small parameter $V=0.01$. In both cases, we can see that there is always one resonant peak.

and 3(b), there is one resonant peak at $E=1.5$ and $E=3.0$, respectively, while in Fig. 3(c), no resonant peak is found. One can easily explain these numerical results with the help of Eq. (6). When $\Phi=0$, from Eq. (19), the possible resonant energies are $E_1^s=2\varepsilon_a-\varepsilon_b$ and $E_2^s=\varepsilon_b$, by the definition of the transfer matrix of Eq. (14), E_2^s is unallowed, consequently, only E_1^s remains. For the case (a), where the energy band is $[-1.5,2.5]$ and the resonant energy $E_1^s=1.5$, it is evident that this energy lies in the energy band; for case (b), the energy band is $[-1.0,3.0]$ and the resonant energy $E_1^s=3.0$, which happens to lie at the right edge of energy band, so the transmission behavior still can be observed; for case (c), the energy band is $[-0.9,3.1]$, obviously, the resonant energy $E_1^s=3.3$ will lie outside the permitted range, thus leading to a nontransmitting behavior of Fig. 3(c).

In Fig. 4 we aim to show the effect of magnetic flux on the transmission spectrum of Fig. 3(a). Four different values of Φ/Φ_0 are considered. As shown in Fig. 4(a), for a rather small value of $\Phi/\Phi_0=0.02$, we have two resonant peaks at $E_1^s=0.5+\sqrt{1+4\sin^2(0.02\pi)}\approx 1.5079$ and $E_2^s=0.5-\sqrt{1+4\sin^2(0.02\pi)}\approx -0.5079$, which is different from the one energy peak of Fig. 3(a). From this result, it seems that the magnetic field does not destroy the symmetry of the mesoscopic ring defects, furthermore, some resonant peaks can be excited by the threading magnetic field. Figures 4(b) and 4(c) show the results for $\Phi/\Phi_0=0.2$, and $\Phi/\Phi_0=0.33$, respectively. The corresponding peaks can also be determined by Eq. (19). From these figures, it is easy to see that as the value of Φ/Φ_0 increases, two resonant peaks will move toward the band edges of the studied system ($E_L=-2V+\varepsilon_a$ and $E_R=2V+\varepsilon_a$). Finally, in the case $\Phi/\Phi_0=0.35$, there is no resonant peak in the figure [see Fig. 4(d)], in this case $W=0.5$ and $\cos(\gamma/2)\approx 0.454$, then $W>\cos(\gamma/2)$, which does not meet the condition of Eq. (21), consequently, there is no resonant peak in the corresponding system. Our numerical results agree very well with the theoretical predictions.

B. Many siamese-twins-like mesoscopic ring defects

By applying Eq. (11) again, we calculate the transmission coefficient as a function of energy for the system of Fig. 1(b). This is analogous to Figs. 3 and 4 for the SMR systems. First, in the absence of magnetic flux, Fig. 5(a) displays the numerical result for system with parameters $V=1.0$, $\varepsilon_a=0.5$, and $\varepsilon_b=-0.5$. Then $W=0.5>0$, from Eqs. (30) and (32), and the corresponding resonant energies are $E_1^{st}=2\varepsilon_a-\varepsilon_b=1.5$, and $E_3^{st}=\sqrt{17}/2\approx 2.0616$. It should be noted that there are two not allowed resonant energies: $E_2^{st}=\varepsilon_b=-0.5$, and $E_4^{st}=-\sqrt{17}/2\approx -2.0616<-2V+\varepsilon_a=-1.5$. Figure 5(b) for $V=1.0$, $\varepsilon_a=1.0$, and $\varepsilon_b=-1.0$, is similar to case (a), the positions of the perfect transmission peaks are at $E_1^{st}=2\varepsilon_a-\varepsilon_b=3.0$, and $E_3^{st}=\sqrt{20}/2\approx 2.2361$. For the sake

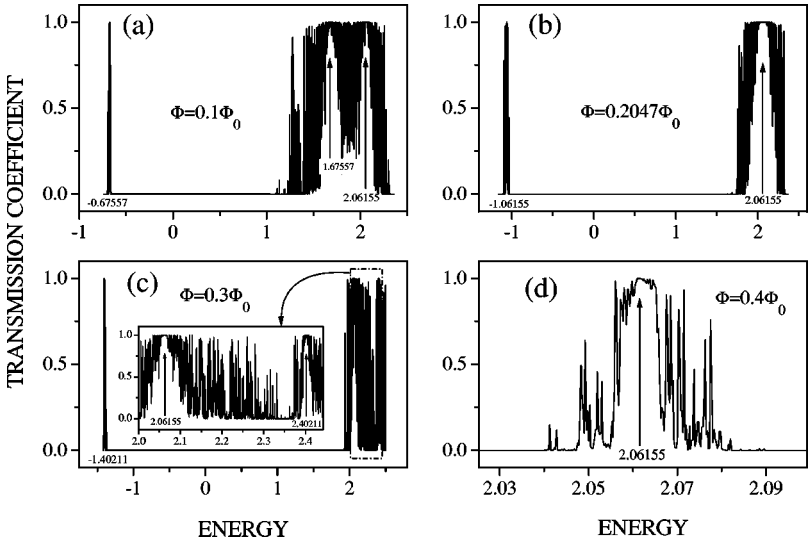

FIG. 6. Transmission coefficients as a function of energy for the STMR defect system of Fig. 1(b) for different magnetic flux Φ. Other parameters are same with these in Fig. 5(a). (a) $\Phi=0.1\Phi_0$, (b) $\Phi\approx 0.2047\Phi_0$, (c) $\Phi=0.3\Phi_0$, and (d) $\Phi=0.4\Phi_0$. Note that there is always one resonant peak $E\approx 2.061\,55$ in these figures. In (a) and (c) there are three resonant peaks, and in (b) (a special case), one of the resonant energies is doubly degenerate, therefore, only two resonant peaks appear in this figure, in (d) two resonant peaks disappear, and only the magnetic-field-independent resonant peak $E\approx 2.061\,55$ remains.

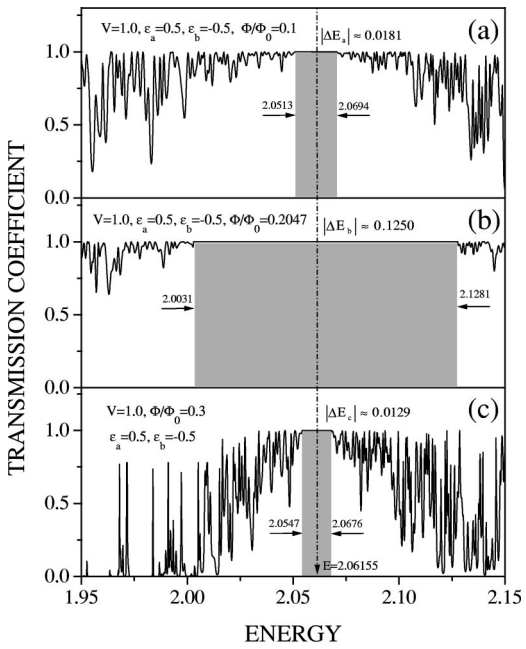

FIG. 7. Some enlarged figures of Fig. 6 around the energy $E \approx 2.061\,55$. (a) before the resonant energy, the width of the perfect transmission region is $|\Delta E_a| \approx 0.0181$, (b) the resonant phenomenon happens, the width of the perfect transmission region is $|\Delta E_b| \approx 7|\Delta E_a|$, (c) after resonant energy, the width of the perfect transmission region is $|\Delta E_c| \approx 0.1|\Delta E_b|$.

of demonstration of the analytical conclusion: for any given W, there is always one energy where the transmission coefficient is unity. We numerically obtain two figures [Figs. 5(c) and 5(d)] with some special values of system parameters. In Fig. 5(c) for $V=1.0$, $\varepsilon_a=10.0$, and $\varepsilon_b=-10.0$, and in Fig. 5(d) for $V=0.01$, $\varepsilon_a=0.5$, and $\varepsilon_b=-05$. These two figures show clearly that there is one resonant peak at $E_3^{st} = 0.5\sqrt{20^2+16} \approx 10.198$, and $E_3^{st} = 0.5\sqrt{1+16*0.01^2} \approx 0.500\,400\,3$, respectively.

Second, when the magnetic flux $\Phi \neq 0$, it is found that the positions and the number of resonant peaks are dependent on the choice of the magnetic flux Φ. Except for the magnetic flux, the parameters of Fig. 6 are same as those of Fig. 5(a). As can be seen in Fig. 6(a), when $\Phi = 0.1\Phi_0$, there are three resonant peaks which are analytically determined by $E_1^{st} = 0.5 + \sqrt{1+4\sin^2(0.1\pi)} \approx 1.675\,57$, $E_2^{st} = 0.5 - \sqrt{1+4\sin^2(0.1\pi)} \approx -0.675\,57$, and $E_3^{st} = 0.5\sqrt{17} \approx 2.061\,55$. We plot Fig. 6(b) with $\Phi = \arccos(0.5\sqrt{4.25} - 0.75)\Phi_0 \approx 0.2047\Phi_0$ which is given by Eq. (39), we find that there are only two perfect transmission peaks. In fact, in this special case, there is one doubly degenerate resonant energy ($E_1^{st} = E_3^{st}$). When $\Phi > \arccos(0.5\sqrt{4.25} - 0.75)\Phi_0$, the degenerate resonant peak will separate into two resonant peaks, this phenomenon is shown in Fig. 6(c) for $\Phi = 0.3\Phi_0$. Finally, when $\Phi = 0.4\Phi_0$, two magnetic-flux-dependent resonant peaks disappear, consequently, only the magnetic-flux-independent resonant peak $E_3^{st} \approx 2.06155$ is kept in Fig. 6(d).

To examine in detail the ''resonant'' behavior ($E_1^{st} = E_3^{st}$), we replot the transmission coefficient versus energy picture around $E = E_3^{st} = 0.5\sqrt{17} \approx 2.0616$ for three cases, (a) $\Phi/\Phi_0 = 0.1$, (b) $\Phi/\Phi_0 = 0.2047$, and (c) $\Phi/\Phi_0 = 0.3$. For the sake of clear visualization, the perfect transmission regions are marked by light gray in these figures. We can see that, at the special value of flux $\Phi \approx 0.2047\Phi_0$, the perfect transmission region is much wider than those of Figs. 7(a) and 7(c). Approximately, we give following relations: $|\Delta E_b| \approx 7|\Delta E_a|$ and $|\Delta E_b| \approx 10|\Delta E_c|$.

V. SUMMARY AND DISCUSSIONS

We have investigated the transmission coefficients in one-dimensional random lattices with mesoscopic ring defects. The considered defects are (a) squarelike mesoscopic ring (SMR) defects, and (b) siamese-twins-like mesoscopic ring (STMR) defects. Theoretically, for the special case of one SMR defect, we demonstrated there are two magnetic-flux-Φ-dependent complete transmission peaks ($T=1$), which will appear or disappear at the same magnetic flux. For the case of one STMR defect, we predicted some interesting behaviors of transmission coefficients, such as the magnetic-flux dependent and independent transmission peaks and the ''resonant'' phenomenon in the studied system. We have successfully given the condition under which the ''resonant'' phenomenon can be observed.

To explicitly test the analytical results, we studied the same problem numerically for the systems with many SMR or STMR defects. Among these investigations, we plotted some figures of transmission spectra for the cases with magnetic flux $\Phi = 0$ and $\Phi \neq 0$, respectively. With these comparisons, we can conclude that the magnetic field influences indeed the transmission properties of the studied systems, furthermore, some complete resonant peaks can be excited by the magnetic field. Therefore, we can conclude that the magnetic field does not destroy the symmetry of the mesoscopic ring defects.

We also studied the ''resonant'' phenomenon that happen in the STMR systems. We presented the figure which shows clearly this behavior. The study of the influence of the magnetic field on the electron transportation is an interesting topic. There are still a lot things to be done, for instance, different structure of mesoscopic rings, different distribution of magnetic field, etc.

[1] *Mesoscopic Phenomena in Solids*, edited by B.L. Altshuler, P.A. Lee, and R.A. Webb (North-Holland, New York, 1991).
[2] H.L. Engquist and P.W. Anderson, Phys. Rev. B **24**, 1151 (1981).
[3] M. Büttiker, Y. Imry, and R. Landauer, Phys. Lett. **96A**, 365 (1983).
[4] Y. Geven, Y. Imry, and M.Y. Azbel, Phys. Rev. Lett. **52**, 129 (1984).
[5] M. Heiblum, M. Nathan, D. Thomas, and C. Knoedler, Phys. Rev. Lett. **55**, 2200 (1985).
[6] R. Landauer and M. Büttiker, Phys. Rev. Lett. **54**, 2049 (1985).

[7] U. Sivan and Y. Imry, Phys. Rev. B **33**, 551 (1986).
[8] O. Entin-Wohlman, C. Hartzstein, and Y. Imry, Phys. Rev. B **34**, 921 (1986).
[9] M. Cahay, S. Bandyopadyay, and H.L. Grubin, Phys. Rev. B **39**, 12 989 (1989).
[10] H.F. Cheung, E.K. Riedel, and Y. Gefen, Phys. Rev. Lett. **62**, 587 (1989).
[11] L.P. Levy, G. Dolan, J. Dunsmuir, and H. Bouchiat, Phys. Rev. Lett. **64**, 2074 (1990).
[12] V. Ambegaokar and U. Eckern, Phys. Rev. Lett. **65**, 381 (1990).
[13] C.H. Wu and G. Mahler, Phys. Rev. B **43**, 5012 (1991).
[14] J. Xia, Phys. Rev. B **45**, 3593 (1992).
[15] A. Aldea, P. Gartner, and I. Corcotoi, Phys. Rev. B **45**, 14 122 (1992).
[16] W. Deng, Y. Liu, and C. Gong, Phys. Rev. B **50**, 7655 (1994).
[17] D. Takai and K. Ohta, Phys. Rev. B **48**, 1537 (1993); **50**, 18 250 (1994).
[18] M. Abraham and R. Berkovits, Phys. Rev. Lett. **70**, 1509 (1993).
[19] Richard Berkovits and Yshai Avishai, Phys. Rev. Lett. **76**, 291 (1996).
[20] B. Doucot and R. Rammal, Phys. Rev. Lett. **55**, 1148 (1985).
[21] F. Oppen and E.K. Riedel, Phys. Rev. Lett. **66**, 88 (1991).
[22] D.S. Golubev and A.D. Zaikin, Phys. Rev. Lett. **81**, 1074 (1998).
[23] Daisuke Takai and Kuniichi Ohta, Phys. Rev. B **50**, 2685 (1994).
[24] Zhiwen Pan, Shijie Xiong, and Changde Gong, Phys. Rev. E **58**, 2408 (1998).
[25] Youyan Liu, Honglin Wang, Zhaoqing Zhang, and Xiujun Fu, Phys. Rev. B **53**, 6943 (1996).
[26] Youyan Liu and P.M. Hui, Phys. Rev. B **57**, 12 994 (1998).
[27] A. Yacoby, M. Heiblum, D. Mahalu, and H. Shtrikman, Phys. Rev. Lett. **74**, 4047 (1995).
[28] G. Hackenbroich and H.A. Weidenmüller, Phys. Rev. Lett. **76**, 110 (1996).
[29] J. Wu *et al.*, Phys. Rev. Lett. **80**, 1952 (1998).
[30] Kicheon Kang, Phys. Rev. B **59**, 4608 (1999).
[31] P.W. Anderson, Phys. Rev. **109**, 1492 (1958).
[32] D.H. Dunlap, H.-L. Wu, and P. Phillips, Phys. Rev. Lett. **65**, 88 (1990).
[33] P. Phillips and H.-L. Wu, Science **252**, 1805 (1991).
[34] H.-L. Wu, W. Goff, and P. Phillips, Phys. Rev. B **45**, 1623 (1992).
[35] S.N. Evangelou and E.N. Economou, J. Phys. A **26**, 2803 (1993).
[36] C.M. Soukoulis, M.J. Velgakis, and E.N. Economou, Phys. Rev. B **50**, 5110 (1994).
[37] Riccardo Farchioni and Giuseppe Grosso, Phys. Rev. B **56**, 1170 (1997).
[38] B.L. Burrows and K.W. Sulston, Phys. Rev. B **51**, 5732 (1995).